

Supporting Information

MicroRNA-Guided Selective Release of Loads from Micro/Nano Carriers Using Auxiliary Constitutional Dynamic Networks

*Pu Zhang,^a Liang Yue,^a Margarita Vázquez-González,^a Zhixin Zhou,^a Wei-Hai Chen,^a Yang
Sung Sohn,^b Rachel Nechushtai,^b and Itamar Willner^{a,*}*

^aInstitute of Chemistry, Center for Nanoscience and Nanotechnology, The Hebrew University
of Jerusalem, Jerusalem 91904, Israel.

^bInstitute of Life Science, The Hebrew University of Jerusalem, Jerusalem 91904, Israel.

E-mail: willnea@vms.huji.ac.il

EXPERIMENTAL SECTION

Materials and Instruments. 2-[4-(2-Hydroxyethyl)piperazin-1-yl]ethanesulfonic acid sodium salt (HEPES), sodium chloride, magnesium chloride, calcium chloride, sodium carbonate, doxorubicin hydrochloride (DOX), camptothecin (CPT), 4-carboxyphenylboronic acid, dextran (40 kDa), carboxymethyl cellulose (CMC) (90 kDa), N-(3-dimethylaminopropyl)-N'-ethylcarbodiimide hydrochloride (EDC), N-hydroxysulfosuccinimide sodium salt (sulfo-NHS), N,N-Dicyclohexylcarbodiimide (DCC), 4-(Dimethylamino)pyridine (DMAP), N, N, N', N'-tetramethylethylenediamine (TEMED), acrylamide solution (40%), poly(-allylamine hydrochloride) (PAH, 58 kDa), ethylenediaminetetraacetic acid disodium salt dihydrate (EDTA), 2,5-Dibromoaniline, 4-(methoxycarbonyl)-phenylboronic acid, cesium fluoride (CsF), anhydrous tetrahydrofuran (THF), dimethylformamide (DMF), palladium(II) acetate (Pd(OAc)₂), dibenzocyclooctyne-sulfo-N-hydroxysuccinimidyl ester (DBCO-sulfo-NHS), triphenylphosphine (PPh₃), tert-butyl nitrite (tBuONO), azidotrimethylsilane (TMSN₃), and zirconium tetrachloride were bought from Sigma-Aldrich. DNA oligonucleotides were synthesized and purified at Integrated DNA Technologies Inc. (Coralville, IA). SYBR Gold nucleic acid gel stain was purchased from Invitrogen. Ultrapure water from NANOpure Diamond (Barnstead) source was applied throughout the whole experiments.

A Magellan XHR 400L scanning electron microscope (SEM) and an FV-1000 confocal microscope (Olympus, Japan) were employed to characterize the microcarriers. Fluorescence spectra was measured with a Cary Eclipse Fluorometer (Varian Inc.). The excitation of FAM, ROX, Cy5 and Cy5.5 were measured at 496, 588, 648 and 685 nm. The emission of FAM, ROX, Cy5 and Cy5.5 were performed at 516, 608, 668 and 706 nm, respectively. The excitation of doxorubicin and camptothecin were measured at 480 and 423 nm. The emission of doxorubicin and camptothecin were measured at 590 and 450 nm. The concentration of DNA

oligonucleotides were monitored by UV-2401PC (SHIMADAZU). The gel experiment was run on a Hoefer SE 600 electrophoresis unit.

The sequences of all nucleic acid used in this paper is listed as follows: (from 5' to 3')

A: GATATCAGCGATACGATACAAACATTAGCATTAACGTGCCTTAA

A': ACCCCTATCACGGTTTGTATCGTCCACCCATGTTTCGTCA

B: CTGCTCAGCGATACGATACAAACAATCCTTAA

B': GCATTCACCGGTTTGTATCGTCCACCCATGTTACTCT

T₁-microRNA-155: UAA AUGCUAAUCGUGAUAGGGGU

T₂-microRNA-124: UUAAGGCACGCGGUGAAUGC

A-MOD: GATATCAGCGATACGATACAAACATTAGCATTAACGTGCCTTAACACAC
ACACA

A'-MOD: TCTCTCTCACCCCTATCACGGTTTGTATCGTCACCCATGTTTCGTCA

Sub 1 (AB'): FAM-AGAGTATrAGGATATC-BHQ1

Sub 2 (BA'): ROX-TGACGATrAGGAGCAG-BHQ2

Sub 3 (BB'): CY5-AGAGTATrAGGAGCAG-BHQ2

Sub 4 (AA'): CY5.5-TGACGATrAGGATATC-IBRQ

Sub1-noFQ (AB'): AGAGTATrAGGATATC

Sub2-noFQ (BA'): TGACGATrAGGAGCAG

Sub3-noFQ (BB'): AGAGTATrAGGAGCAG

Sub4-noFQ (AA'): TGACGATrAGGATATC

H₁: CCGGAGTATTGCGGTTCCAGAGTATrAGGAGCAGCCTTCCTGGCGGACCGCA
ATACTCCGGGCTGCCCCCAGG

H₂: TTCCAGACAAGAGTGCCATTGACGATrAGGAGCAGTACCCTGTAGCGGCACT
CTTGTCTGGACCGGGACGGAA

p'/L₁, (9): GGAGCAGCCTTCCTGGCGGACCGCAATACTCCGGGCTGCCCCCAGG

q'/L₂, (10): GGAGCAGTACCCTGTAGCGGCACTCTTGTCTGGACCGGGACGGAA

(1): GAATCGATTACCCCCAGG

(2)/p: TCGATTCCCTGGGGGCAGCCCGGAGTATTGCGGTCCGCCAGGAAGGTAGTT
GGT

(3): CCTTCCTTTTACCAACTA

(4): CTACTATAATGACGGCC

(5)/q: ATAGTAGGGCCGTCCCGGTCCAGACAAGAGTGCCGCTACAGGGTATAAG
AAT

(6): TACCCTGTAAATTCTTA

(7): NH₂-(CH₂)₆-GGAGCAGCCTTCCTGGCGGACCGCAATACTCCGGGCTGC

(7'): CCTGGGGGCAGCCCGGAGTATTGCGGTCCGCCAGGAAGGCTGCTCC

(8): NH₂-(CH₂)₆-GGAGCAGTACCCTGTAGCGGCACTCTTGTCTGGACCGG

(8'): TTCCGTCCCGGTCCAGACAAGAGTGCCGCTACAGGGTACTGCTCC

Additionally, the ribonucleobase cleavage site of **rA** in all the substrates of the different Mg²⁺-dependent DNazymes is marked in bold, the sequences of corresponding Mg²⁺-dependent DNzyme are indicated with underline.

Generation of CDNs. The [2×2] CDN “S” depicted in Figure 1, consisted of the constituents AA', AB', BA' and BB', was prepared as follows. A mixture of A, A', B and B' (2 μM each) in HEPES buffer (10 mM, 20 mM MgCl₂, pH = 7.2) was annealed at 65 °C for 15 min, subsequently, cooled down to 25 °C with the rate of 0.33 °C minute⁻¹, and eventually allowed to equilibrate at 25 °C for 2 hours, yielding CDN “S”. For the conversion of CDN “S” to CDN “X” or CDN “Y”, the mixture of AA', AB', BA' and BB' (CDN “S”, 1 μM) was brought to the corresponding trigger miRNA-155 or miRNA-124 (1.3 μM), and was allowed to equilibrate at 33 °C for 12h, to generate CDN “X” or CDN “Y”, respectively.

Quantifying the constituents of CDNs. 100 μL of the equilibrated mixture of AA', AB', BA' and BB' (CDNs) was subjected to respective substrates modified with fluorophore/quencher pairs while the other substrates lacked modification (noFQ). For instance, to quantify the concentration of AB', 100 μL of the equilibrated mixture of CDNs (1 μM) was incubated with the sub1, sub2-noFQ, sub3-noFQ and sub4-noFQ, 5 μL of 100 μM each. Subsequently, the time-dependent fluorescence changes produced by the cleavage of sub1 by the Mg^{2+} -dependent DNzyme associated with the AB' were monitored. Based on the appropriate calibration curve corresponding to the rates of cleavage of the corresponding substrates by different concentrations of the intact constituents, the concentrations of the constituents in the different CDNs were probed.

Synthesis of doxorubicin-dextran (DOX-D). The synthesis of DOX-D is followed as described previously³² and the details is shown as follows. Doxorubicin was pre-modified with 4-carboxyphenylboronic acid *via* EDC/NHS reaction coupling followed by the binding of the boronic acid to dextran to yield the respective boronic ester. EDC (0.8 mg, 4.1 μmole) and sulfo-NHS (2.2 mg, 10.1 μmole) were added to 1.4 mL of 0.5×10^{-3} M 4-carboxyphenylboronic acid solution (dissolved in 10×10^{-3} M HEPES, containing 500×10^{-3} M NaCl, pH 7) and the above mixture was treated at room temperature for 15 min. Next, 100 μL of 10×10^{-3} M doxorubicin was introduced to the mixed solution that was allowed to continuous shake at room temperature for 2 h, incubating at 4 $^{\circ}\text{C}$ overnight. Subsequently, 2 mL of dextran solution (0.08 mg mL^{-1} in 10×10^{-3} M HEPES, pH 10) was added to the mixture that was further allowed to react at room temperature for 2 h while shaking and incubated overnight at 4 $^{\circ}\text{C}$. The obtained product was purified and separated from free doxorubicin using a centrifugal filter device (Amicon, 10K MWCO). After centrifugation, the resulted DOX-D was collected and stored at 4 $^{\circ}\text{C}$ for further use. Solubilization of the DOX-D (0.28 mg) in 100 μL of water generates a 40×10^{-6} M DOX-D solution. The concentration of the DOX-D solution was determined by the

hydrolysis of DOX-D at pH 5, measuring the fluorescence intensity of the released Dox. On the basis of an appropriate calibration curve corresponding to the fluorescence of known concentrations of DOX, the amount of the released DOX could be calculated.

Synthesis of camptothecin-CMC (CPT-CMC). The schematic synthesis of CPT-CMC is shown in Figure S23. 200 mg of CMC, 0.29g of CPT, 0.206g of DCC and 1 mg of DMAP were mixed in methylene dichloride and reacted overnight under continuously stirring. Then the mixture was washed with water in centrifugal filter device (Amicon, 10K MWCO) to remove the unreacted reagents. The final supernatant was collected and stored at 4 °C for further use.

Preparation of CaCO₃ microparticles and their encapsulation. The proposed microcapsules were prepared with microparticle of CaCO₃ templates by the previous procedure³² while applying new loads for incorporation into the microcapsules. Briefly, CaCO₃ microparticles were loaded with DOX-D or CPT-CMC (0.3 mg mL⁻¹, each). The loaded microparticles were centrifuged (900 rpm, 20 s) very carefully and followed by washing the particles to remove non-adsorbed loads. The resulting loaded CaCO₃ cores serves as templates to fabricate the microcapsules.

Assembly of layer-by-layer DNA stabilized microcapsules: The capsules were prepared as described previously³². For the preparation of the MC-1 bridged by DNA “p”, two kinds of DNA shells, (1)/(2) and (2)/(3) were prepared and stored at 25 °C before use. The nucleic acids of (1) and (2) with the final concentration of 10×10^{-6} M and 5×10^{-6} M were annealed at 80 °C for 10min and were transferred to incubator (25 °C). Accordingly, 10×10^{-6} M of (3) and 5×10^{-6} M of (2) were also annealed at 80 °C and transferred to incubator (25 °C). CaCO₃ templates (6.0 mg) were suspended in 300 μL of 1 mg mL⁻¹ PAH solution (in 10×10^{-3} M HEPES, including 500×10^{-3} M NaCl and 50×10^{-3} M MgCl₂, pH 8) for electrostatic adsorption around 30 min. Then, the solution was washed with 10×10^{-3} M HEPES buffer (including 500×10^{-3} M NaCl, pH 8) followed by precipitation of the particles (900 rpm for 20 s). The resulting

PAH-modified CaCO₃ microparticles were coated sequentially with the DNA hybrids (1)/(2) or (2)/(3) for a time-interval of 30 min. After each adsorption step, the particles were subjected to washing procedure to remove non-adsorbed DNA. Six layers of nucleic acids duplex were assembled on CaCO₃ particles. The prepared microcapsules (6.0 mg), were suspended in 10×10⁻³ M HEPES solution (containing 500 × 10⁻³ M NaCl, pH 8). Subsequently, 120 μL of 0.5 M EDTA solution, pH 8, was added to the microcapsules. The dissolution of the CaCO₃ core was allowed to proceed for a time-interval of 1 h. After the suspension became clear, the supernatant EDTA solution was removed by careful centrifugation to avoid aggregation and destruction of the DNA capsules. The capsules were washed three times with 10×10⁻³ M HEPES buffer (containing 500×10⁻³ M NaCl, pH 8) by centrifuging at 500 rpm for 20 min. For the MC-2 bridged by DNA “q”, the nucleic acids of (4) and (5) with the final concentration of 10×10⁻⁶ M and 5×10⁻⁶ M were annealed at 80 °C for 10min and were transferred to incubator (25 °C). 10 ×10⁻⁶ M of (6) and 5×10⁻⁶ M of (5) were also annealed at 80 °C and transferred to 25 °C incubator. The layer-by-layer assembly was followed the same process as MC-1. The number of capsules was counted by an iCyt Eclipse Analyzer Flow Cytometer and it turned out to be ~2000 capsules μL⁻¹.

Preparation of amino-TPDC. Amino-TPDC was prepared on the basis of a previous paper with minor modifications.^{S1} Firstly, 2,5-Dibromoaniline (4.0 mmol, 1.00 g), CsF (19 mmol, 2.91 g) and 4-(methoxycarbonyl)-phenylboronic acid (12.25 mmol, 2.2 g) were dissolved in 50 mL of anhydrous THF in a 100 mL flask under the protection of nitrogen. Next, PPh₃ (3.05 mmol, 0.8 g) and Pd(OAc)₂ (1.35 mmol, 0.30 g) were introduced to the above mixture. The above mixture was then heated at 50 °C for 2 days. The obtained solution was respectively purified by water/dichloromethane extraction and silica gel column chromatography (dichloromethane: ethyl ether = 50: 1 with 0.25% triethylamine). The resulted amino-triphenyldicarboxyl methyl ester (3.32 mmol, 1.2 g) was then suspended in THF and heated to

40 °C. Subsequently, KOH methanol solution (5.5 M, 80 mL) was applied, following by continuous stirring at 40 °C overnight. After centrifugation, a white solid was acquired and was transferred to 10 mL trifluoroacetic acid in 80 mL of THF for 2h at room temperature. The final yellow solid product was achieved by vacuum filtration and washed with THF, methanol, and ether.

Synthesis of NMOFs. The preparation of NMOFs was according to the reported paper.^{S1} First of all, 42 mg of proposed amino-TPDC and 60 mg of ZrCl₄ were mixed together in DMF (100 mL). Then, 5 mL of CH₃COOH was treated with the mixture in an oven and was reacted at 80 °C for 5 days. After that, the obtained NMOFs were centrifuged and washed with DMF, triethylamine/ethanol (1:20, V/V), and ethanol. The concentration of the prepared NMOFs is about to be 0.5 mg mL⁻¹.

Preparation of NMOFs modified with azide group (NMOF-N₃). The dried NMOFs (20 mg) were transferred into 5 mL of THF in a small vial. 1.5 mL of the tBuONO and 1.4 mL of the TMSN₃ were introduced in the same vial. The above solution was then incubated at room temperature for 12h to generate the NMOF-N₃.

Preparation of DBCO-Functionalized DNA (7)/(8). To link DBCO functional groups to nucleic acid (7)/(8), 40 μL of 1×10⁻³ M (7) or (8) was added to 100 μL of 4×10⁻³ M DBCO-sulfo-NHS (dissolved in PBS buffer) and shaken overnight. The obtained solution was filtered with MicroSpin G-25 columns (GE-Heathcare) to produce the pure DBCO-DNA.

Synthesis of DNA (7)/(8)-functionalized NMOFs. Initially, NMOF-N₃ nanoparticles (10 mg, 1 mL) were treated with DBCO-DNA (7)/(8) (100 nmol, 0.5 mL), shaking at 40 °C for 72 h. Then, the above solution was diluted with NaCl to a final concentration of 0.5 M and incubated over 6 h. The DNA (7)/(8)-functionalized NMOFs were washed in PBS buffer for three times to remove unbounded nucleic acids.

The drug loading of NMOFs. To load the drugs, 5 mg of NMOFs were treated with doxorubicin (1.0 mg mL^{-1}) or camptothecin (1.0 mg mL^{-1}) for 24 h in 2 mL of $10 \times 10^{-3} \text{ M}$ PBS buffer ($\text{pH} = 7.4$). The NMOFs were then transferred to a buffer solution and hybridized with nucleic acid (**7'**) or (**8'**), respectively, resulting to the locked state of the duplex DNA modified NMOFs to encapsulate the drugs. 12 h later, the NMOFs were washed several times to remove the unloaded drugs.

Controlling the release of loads from microcapsules or NMOFs using auxiliary CDNs.

The equilibrated CDN “S”, “X” or “Y” ($10 \text{ }\mu\text{L}$, $2 \text{ }\mu\text{M}$) was subjected to the hairpins H_1 or H_2 ($5 \text{ }\mu\text{L}$, $2 \text{ }\mu\text{M}$), and to the prepared solution of microcapsules or NMOFs ($100 \text{ }\mu\text{L}$ for each). The resulting mixture was divided into different batches, each batch was incubated at room temperature for different time-intervals. After incubation, the respective batches were centrifuged at 500 rpm for 20 min to precipitate the residual capsules, and the fluorescence intensity of the released drugs in the supernatant solution was monitored. Notably, all the hairpins were annealed at $95 \text{ }^\circ\text{C}$ and slowly cooled down to room temperature before using.

Cell culture. Human breast cancer cells (MDA-MB-231) were grown in 5% CO_2 RPMI-1640 medium supplemented with 10% FCS, L-glutamine, and antibiotics (Biological Industries). Human liver cancer cell line (HepG2) were grown in 5% CO_2 DMEM medium supplemented with 10% FCS, L-glutamine, and antibiotics (Biological Industries). Normal breast cells (MCF-10A) were maintained in complete growth medium consisting of 1:1 mixture of Dulbecco’s modified Eagle’s medium and Ham’s F12 medium supplemented with horse serum (5%), epidermal growth factor (20 ng/mL), cholera toxin (CT, $0.1 \text{ }\mu\text{g/mg}$), insulin ($10 \text{ }\mu\text{g/mL}$), hydrocortisone (500 ng/mL), and penicillin/streptomycin (1 unit/mL). Cells were plated one day prior to the experiment on 96-well plates for cell viability or on μ -slide 4 well glass bottom (ibidi) for confocal microscopy.

Cell viability experiments. Cell viability was assayed after incubation of the DOX-D loaded microcapsules with or without CDN in MCF-10A, MDA-MB-231 and HepG2 cells planted at a density of 1.2×10^4 cells per well in 96-well plates. CDN “S” and hairpin 1 (H₁)/hairpin 2 (H₂) were co-transfected into the three cells with Lipofectamine 2000 following the protocol provided by the manufacturer. The doses per well of the CDN ingredients and DOX-D load microcapsules were: CDN “S”, AA' 50 μ M; AB' 50 μ M; BA' 50 μ M; BB' 50 μ M; around 26.6k capsules were incubated with 12k cells in each well; average loading of DOX-D per microcapsule: 2.2×10^{-14} mol. After 3 hours incubation with the microcapsules, CDN was added to cells with different hairpins and following 3 hours incubation, cells were washed intensively and then were further incubated for 2 days with growth medium and the cell viability was determined with the fluorescent redox probe, Presto-Blue. The fluorescence of Presto-Blue was recorded on a plate-reader (Tecan Safire) after 1 h of incubation at 37 °C ($\lambda_{ex} = 560$ nm; $\lambda_{em} = 590$ nm).

Confocal microscopy measurements. Cells were planted in μ -slide 4 well glass bottom on one day prior to the experiment. Cells were incubated with the DOX-D loaded microcapsules for 3 hours and then washed with DMEM-Hepes twice. Doxorubicin fluorescence in cells was monitored with the confocal microscopy. Around 200k capsules were incubated with 200k cells in each well.

Table S1. Concentrations of the equilibrated constituents in the different CDNs.

CDN	[AA']/(μM)	[AB']/(μM)	[BA']/(μM)	[BB']/(μM)
S	0.54 ^a (0.51) ^b	0.46 ^a (0.43) ^b	0.53 ^a (0.51) ^b	0.47 ^a (0.48) ^b
X	0.94 ^a (0.92) ^b	0.12 ^a (0.19) ^b	0.10 ^a (0.13) ^b	0.98 ^a (0.94) ^b
Y	0.05 ^a (0.03) ^b	0.92 ^a (0.88) ^b	0.89 ^a (0.92) ^b	0.09 ^a (0.13) ^b

^a Concentration evaluated from the fluorescence change generated by the different DNAzyme reporter units associated with the constituents, and using the appropriate calibration curve.

^b Concentrations evaluated by quantitative electrophoretic separation of the constituents in the different CDNs.

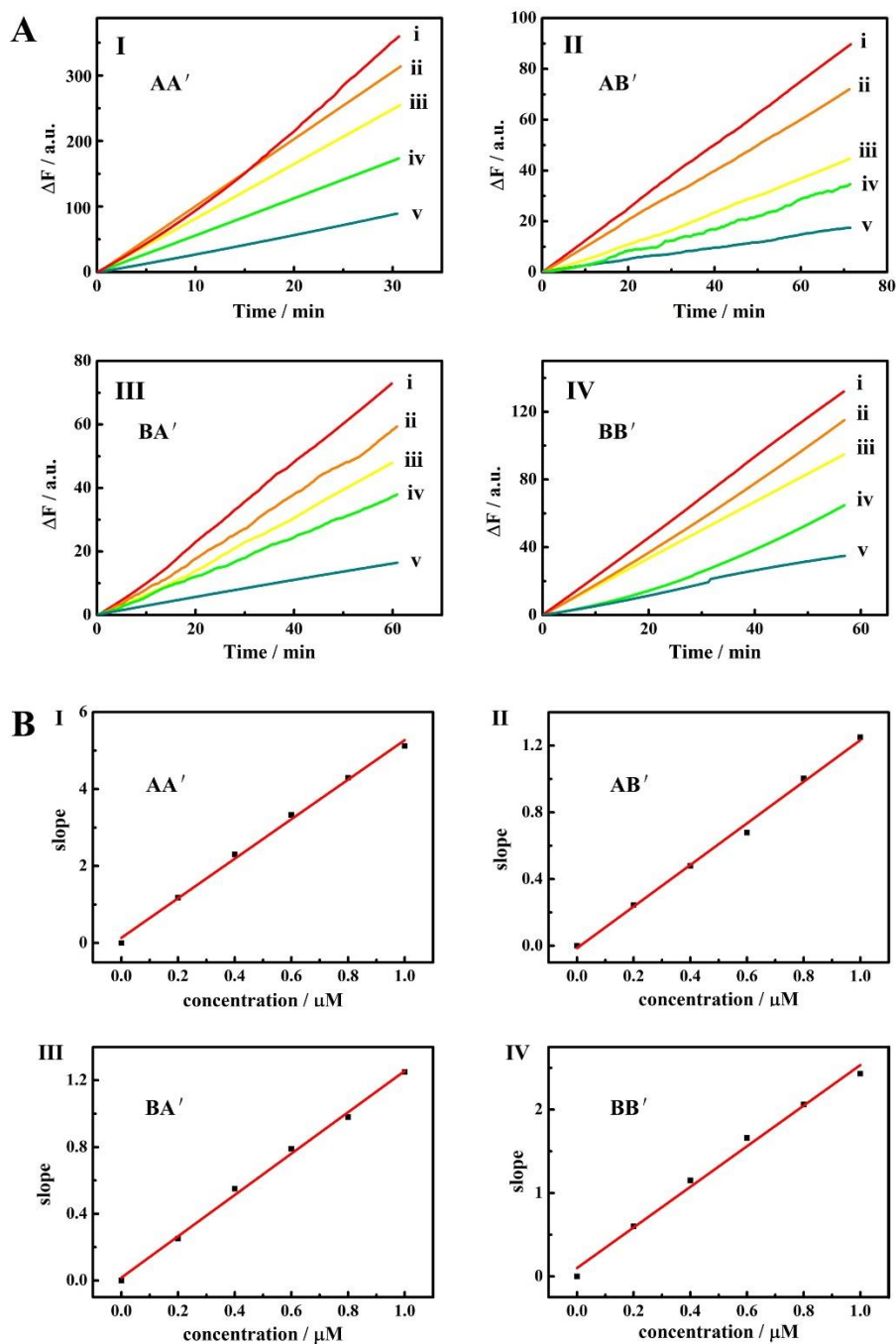


Figure S1. (A) Time-dependent fluorescence changes generated by variable constituents of the DNAzyme reporter units associated with intact structures of the respective constituents. The concentrations of the respective constituents are: (i) 1 μM , (ii) 0.80 μM , (iii) 0.60 μM , (iv) 0.40 μM , and (v) 0.20 μM . (B) Derived calibration curves corresponding to the catalytic activities of the respective DNAzyme reporter units as a function of the concentration of the constituents.

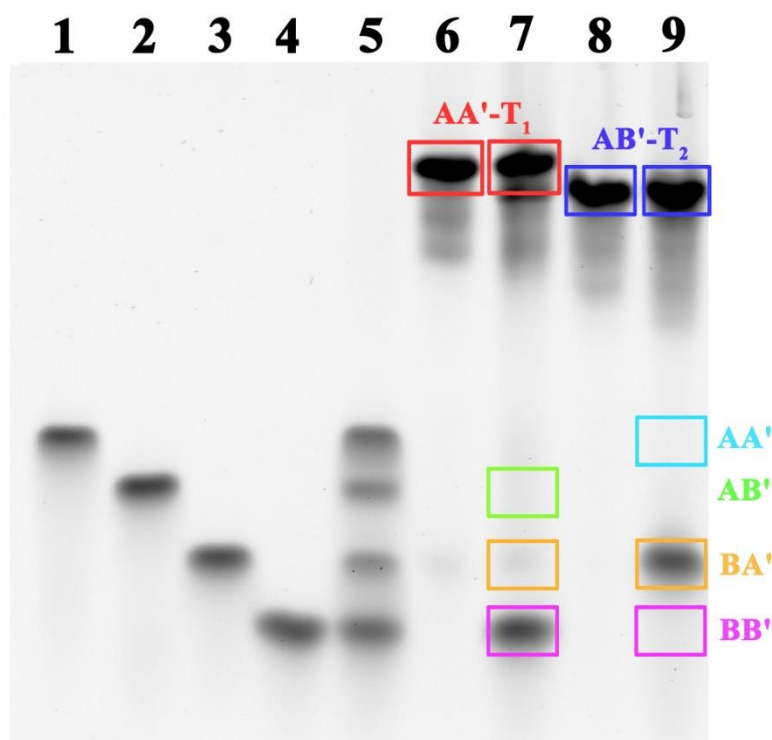


Figure S2. Gel electrophoresis (native PAGE gel, 12%, gel thickness, 1mm) separation of the constituents associated with the different CDNs and quantitative evaluation of the separated constituents. The samples were separated upon applying a 150 V potential, 10 °C (to eliminate the dissociation of duplexes) with a time-interval of 24 h. All of the samples were stained with SYBR Gold and the intensities of different bands were quantitatively analyzed by the ImageJ software by comparing the intensities of the respective separated bands to the intensities developed by the known concentration of the individual reference constituents. Lane 1- Constituent AA' (1 μM). Lane 2-Constituent AB' (1 μM). Lane 3-Constituent BA' (1 μM). Lane 4-Constituent BB' (1 μM). Lane 5-Separated constituents of CDN "S". Lane 6-T₁ stabilized AA' constituent, AA'-T₁ (1 μM). Lane 7-The separated constituents of CDN "X". Note that the constituent AA' by itself is depleted and the band of T₁ stabilized AA', AA'-T₁, is visible. In addition, an intensified band of BB' as compared to CDN "S" is observed, and the band of BA' and AB' are weak, as compared to CDN "S". Lane 8-Intact band of the T₂ stabilized AB' constituent, AB'-T₂. Lane 9-The separated constituents of CDN "Y". Note that the constituents AB' by itself is depleted and the band of T₂ stabilized AB' constituent, AB'- T₂, is visible. Additionally, an intensified band of BA' as compared to CDN "S" is observed, and the bands of AA' and BB' are weak, as compared to CDN "S".

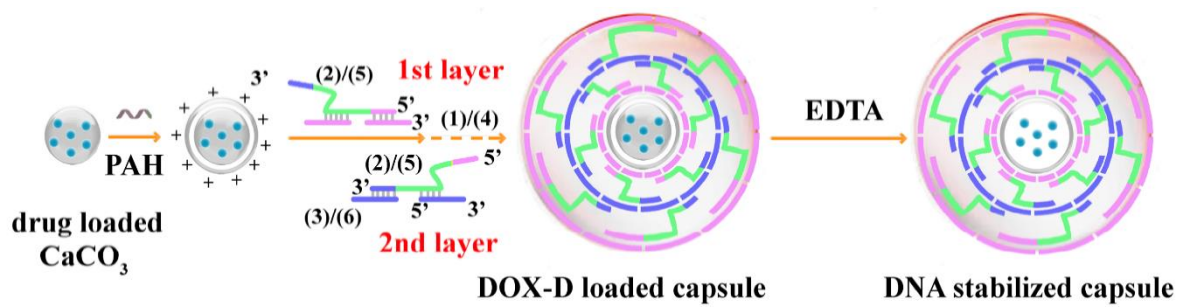


Figure S3. Schematic stepwise synthesis of the drug-loaded stimuli-responsive microcapsules.

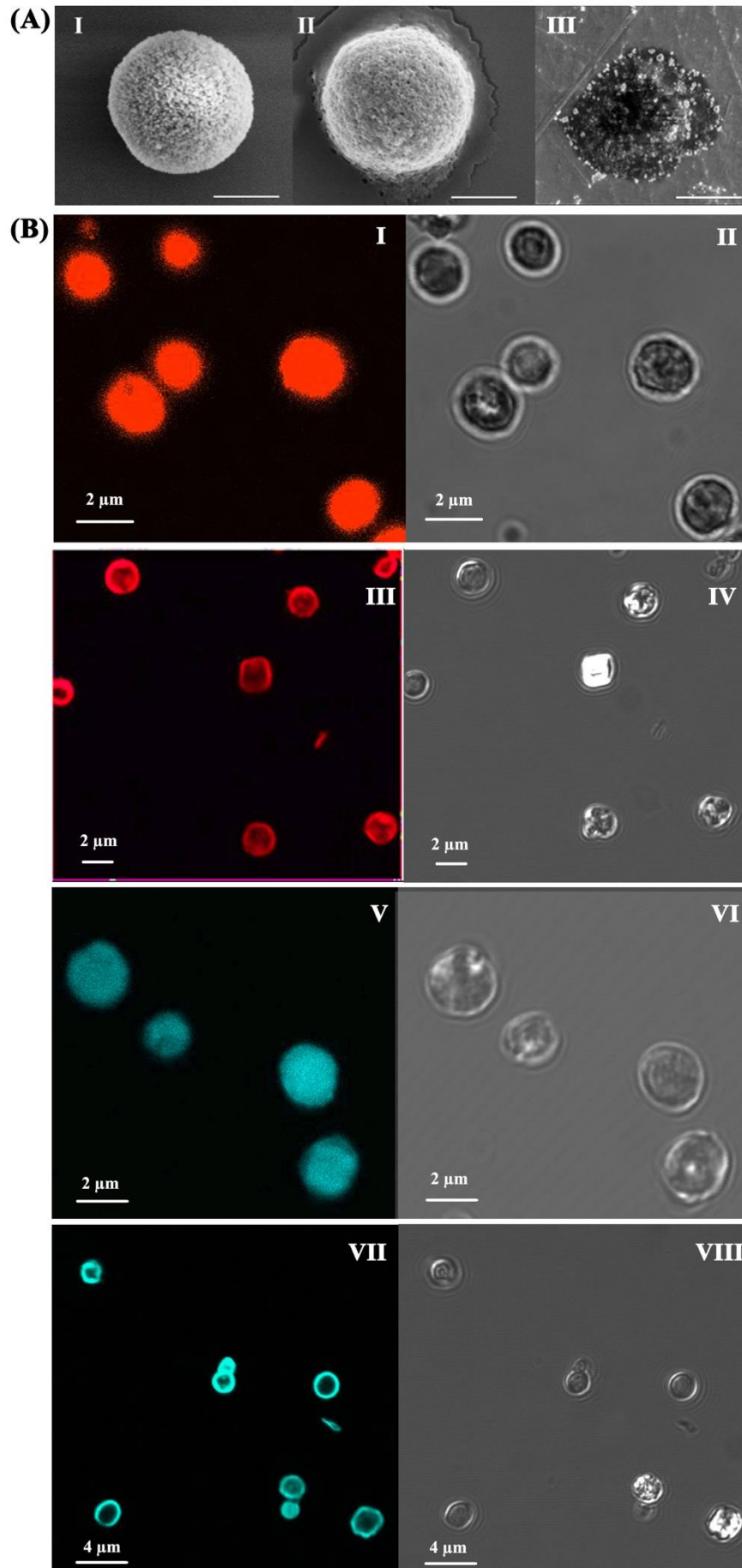


Figure S4. (A) Microscopy images of: Panel I-SEM image of the CaCO₃ microparticle core prior to modification. Panel II-SEM image of the DNA-coated microcapsules. Panel III-SEM image of the DNA-stabilized microcapsules after etching of the CaCO₃ core. (B) Confocal fluorescence microscopy images and bright-field images corresponding to: Panel I and II confocal fluorescence and bright-field images of the DOX-D-loaded particles before etching, and III and IV after etching the core. Panel V and VI confocal fluorescence and bright-field images of the CPT-CMC-loaded particles before etching, and VII and VIII after etching of the core.

Figure S4 (A) exemplifies the SEM images of the bare CaCO₃ microparticles, panel I, the DNA-coated DOX-D loaded CaCO₃ microparticles, panel II, and the microparticles generated upon etching of the CaCO₃ cores, panel III. Figure S4 (B) shows the confocal microscopy fluorescence images and bright-field microscopy images, corresponding to the MC-1 and MC-2 microcapsules. Panels I and II show the fluorescence images (red) and the bright-field images of the DOX-D loaded CaCO₃ microparticles coated with p-bridged nucleic acid shells, respectively. Figure S4 (B), panel III and IV show the fluorescence and bright-field images of the microcapsules after etching off the CaCO₃ core. The microcapsules shrink in their sizes after etching, and the fluorescent DOX-D is detected in the MC-1 inner volume. In addition, Figure S4 (B), panels V and VI show the fluorescence confocal microscopy (green) and bright-field images of the CPT-CMC loaded CaCO₃ microparticles coated with the nucleic acid shells crosslinked by q, respectively. Figure S4 (B) panels VII and VIII show the confocal microscopy and bright-field images of the microcapsules after etching the CaCO₃ cores.

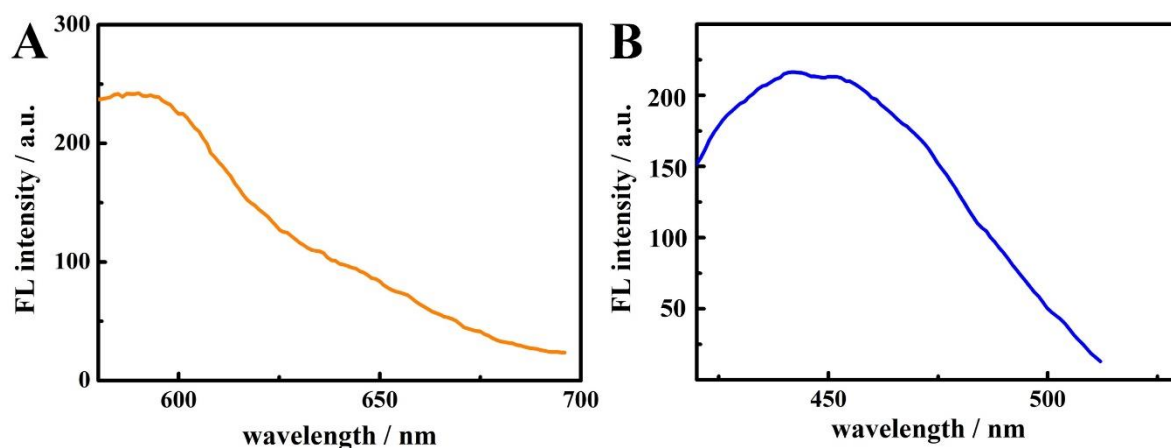


Figure S5. (A) The fluorescence spectra of unbounded DOX after the conjugation of dextran chain and DOX. The mole number of bounded DOX on dextran was calculated according to the mole number of introduced DOX and the unbounded DOX in the solution. Based on the amount of introduced polymer chain, we estimated that the loading of DOX on the dextran carrier was to be 60 DOX units per dextran chain. (B) The fluorescence spectra of unbounded CPT after the conjugation of CPT and CMC. The loading of camptothecin units on the CMC carrier was evaluated the same way and it was calculated to be 45 camptothecin units per polymer chain.

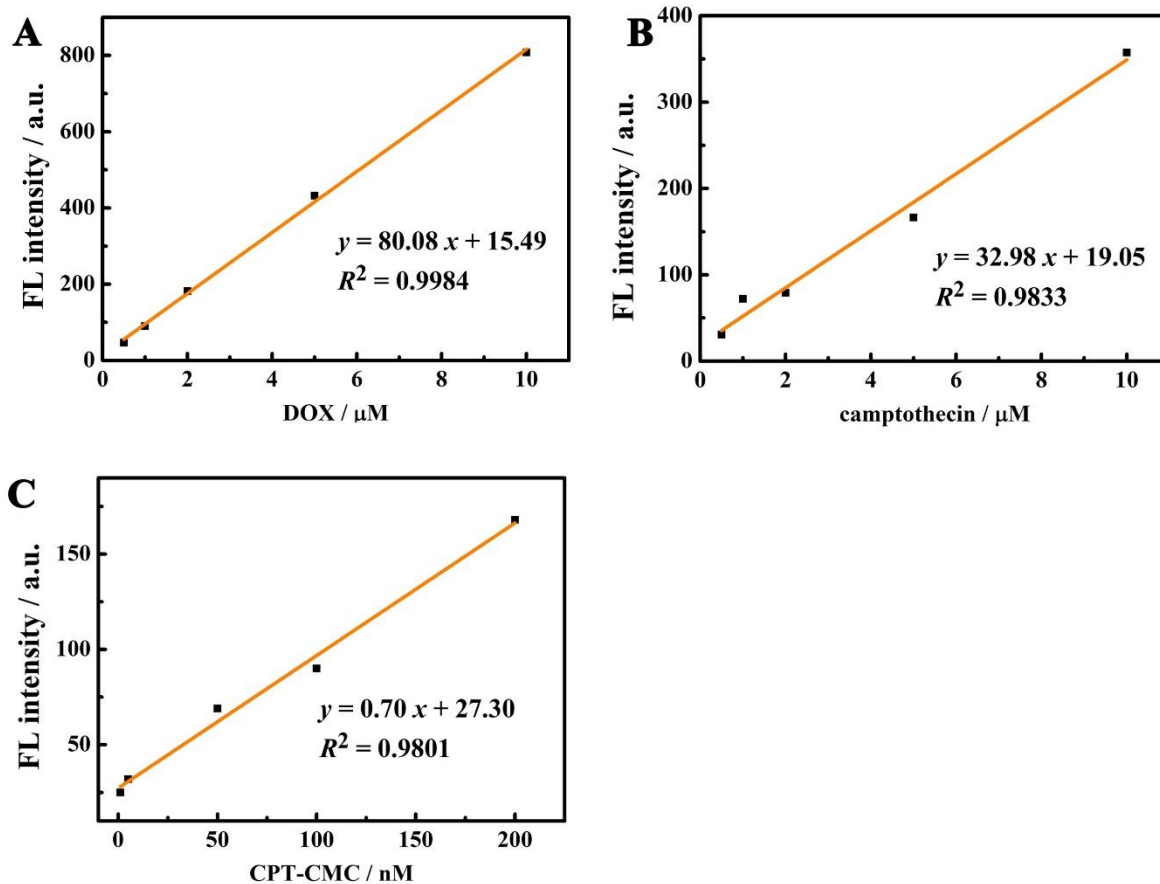


Figure S6. Calibration curves corresponding to (A) doxorubicin, DOX. (B) camptothecin. (C) camptothecin-modified carboxymethyl cellulose, CPT-CMC. The fluorescence of DOX-D was measured after the acidification that allows for the cleavage of doxorubicin from the dextran.

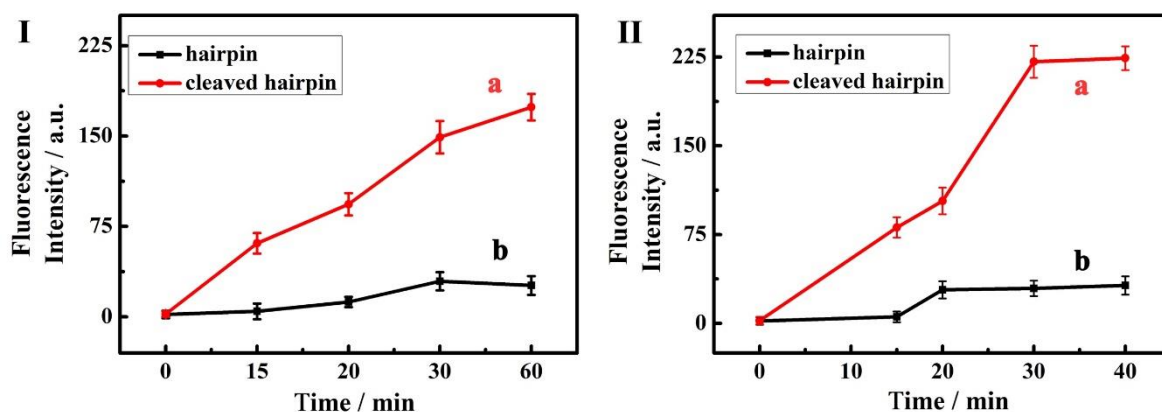


Figure S7. Control experiments demonstrating that the cleavage of the hairpin H_1 is essential to unlock the microcapsules (DOX-D loaded MC-1) and DOX loaded miRNA-155 responsive NMOFs. Panel I: Time-dependent fluorescence changes originating upon the release of DOX-D from the MC-1 capsule upon: (a) Treatment of the capsule with the fragment of the hairpin H_1 , p' . (b) Treatment of the capsules with the intact hairpin H_1 . Panel II: Time-dependent fluorescence changes upon the release of DOX from the miRNA-155 responsive NMOFs upon treatment with: (a) The fragmented hairpin H_1 , L_1 , (9). (b) The intact hairpin H_1 . The results demonstrate the CDN-induced fragmentation of the hairpin H_1 is essential to unlock the drug-loaded MC-1 and the miRNA-155 responsive NMOFs. Error bars derived from $N=3$ experiments.

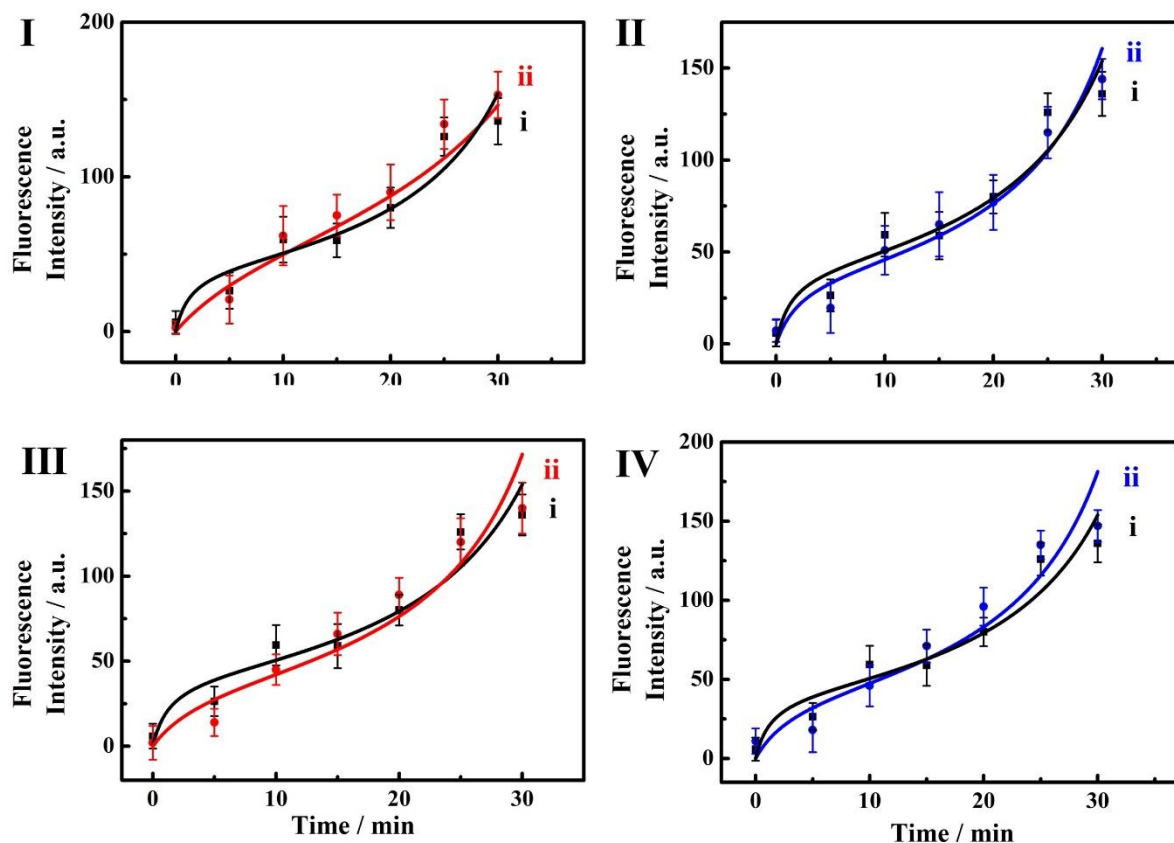


Figure S8. (I) Time-dependent release of DOX-D from the MC-1 microcapsule driven by (i) CDN “S” and (ii) CDN “S” treated with miRNA-145. (II) Time-dependent release of CPT-CMC from the MC-2 microcapsule driven by (i) CDN “S” and (ii) CDN “S” treated with miRNA-145. (III) Time-dependent release of DOX-D from the MC-1 microcapsule driven by (i) CDN “S” and (ii) CDN “S” treated with miRNA-16. (IV) Time-dependent release of CPT-CMC from the MC-2 microcapsule driven by (i) CDN “S” and (ii) CDN “S” treated with miRNA-16. Error bars derived from $N=3$ experiments.

The sequences of the foreign miRNA: (from 5' to 3')

miRNA-145: GUC CAG UUU UCC CAG GAA UCC CU

miRNA-16: UAG CAG CAC GUA AAU AUU GGC G

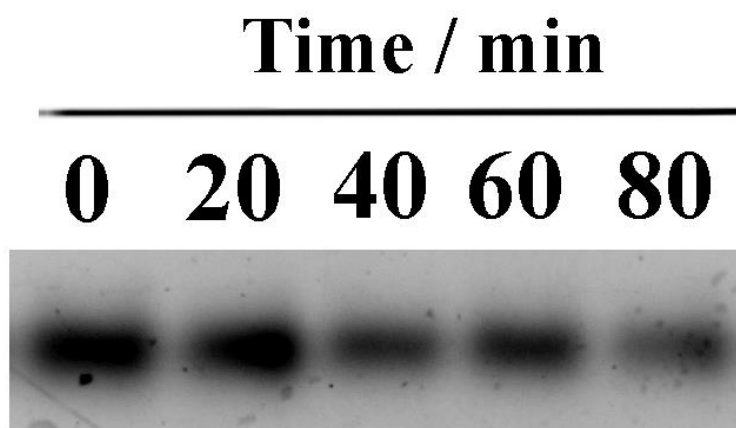


Figure S9. (I) Electrophoresis characterization for the degradation of microcapsule treated with DNase I (0.5U/mL).

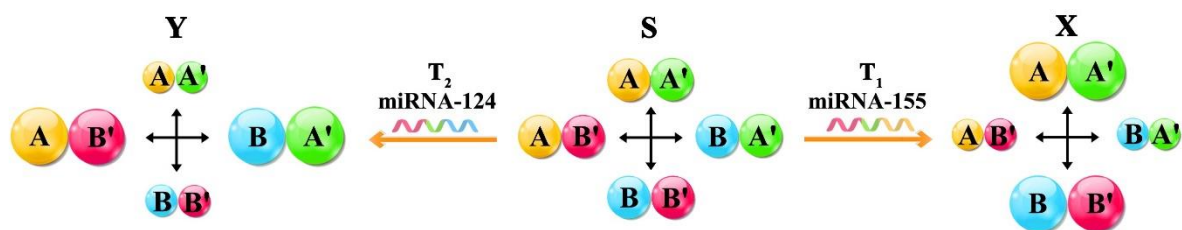


Figure S10. miRNA-guided switching of dynamic constitutional networks consisting of four exchangeable nucleic acid constituents. CDN “S”, CDN “X”, and CDN “Y”.

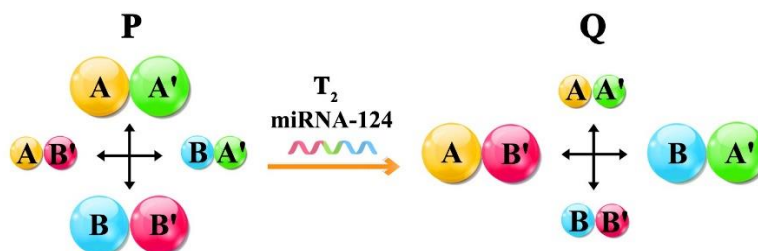


Figure S11. miRNA-124-guided switching of dynamic constitutional networks consisting of four exchangeable nucleic acid constituents. CDN “P” and CDN “Q”.

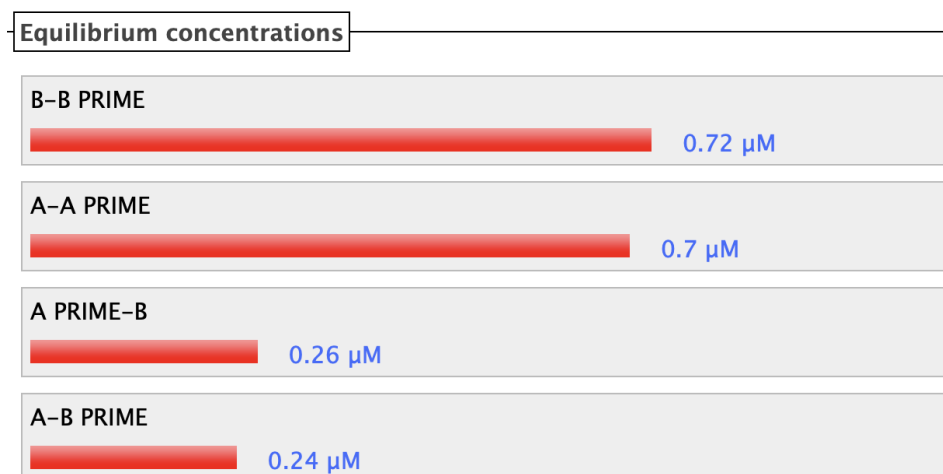


Figure S12. Theoretical concentration value of four constituents (CDN “P”) from NUPACK program.

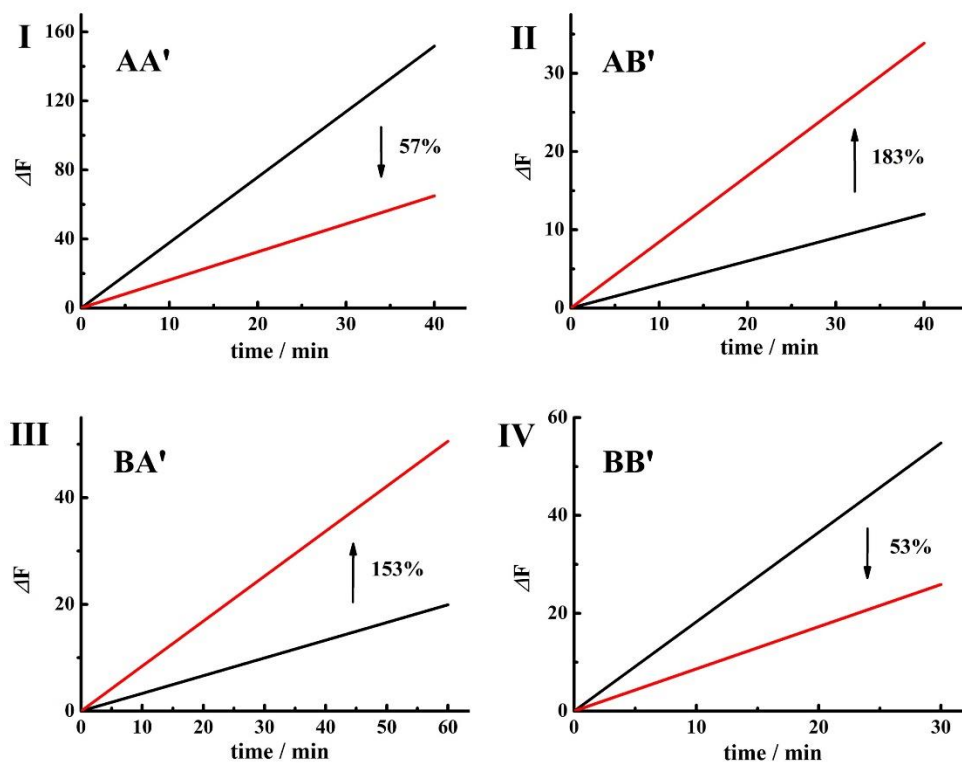


Figure S13. Time-dependent fluorescence changes generated by the DNzyme reporters associated with the different constituents in CDN “P” (black curve) and CDN “Q”, CDN “P” treated with miRNA-124 (red curve). Panel I-constituent AA'; Panel II-constituent AB'; Panel III-constituent BA'; Panel IV-constituent BB'. The percentages of up-regulated/down-regulated contents of the constituents to miRNA driven transitions of CDN “P” to CDN “Q” are indicated in the panels.

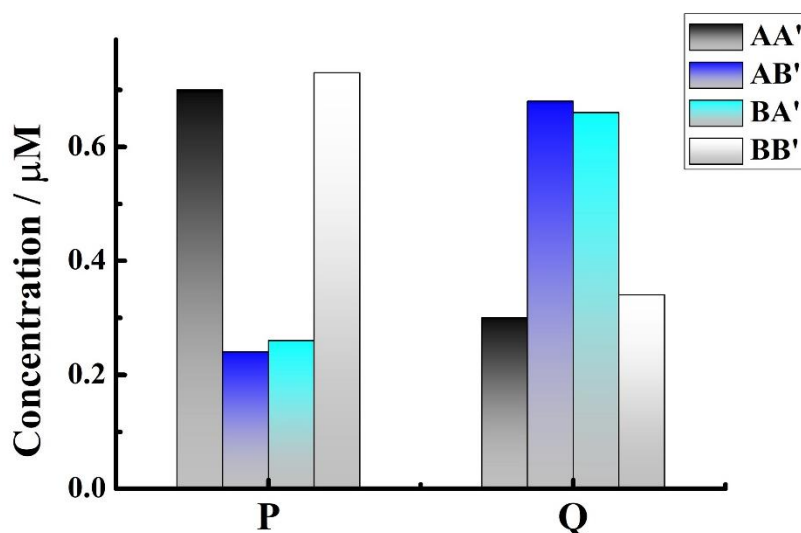


Figure S14. The concentrations of the constituents associated with the CDNs “P” and “Q” shown in Figure 13 (in the form of a bar presentation).

Table S2. Concentrations of the equilibrated constituents in the CDN “P” and “Q”.

CDN	[AA']/(μ M)	[AB']/(μ M)	[BA']/(μ M)	[BB']/(μ M)
P	0.70	0.24	0.26	0.73
Q	0.30	0.73	0.68	0.34

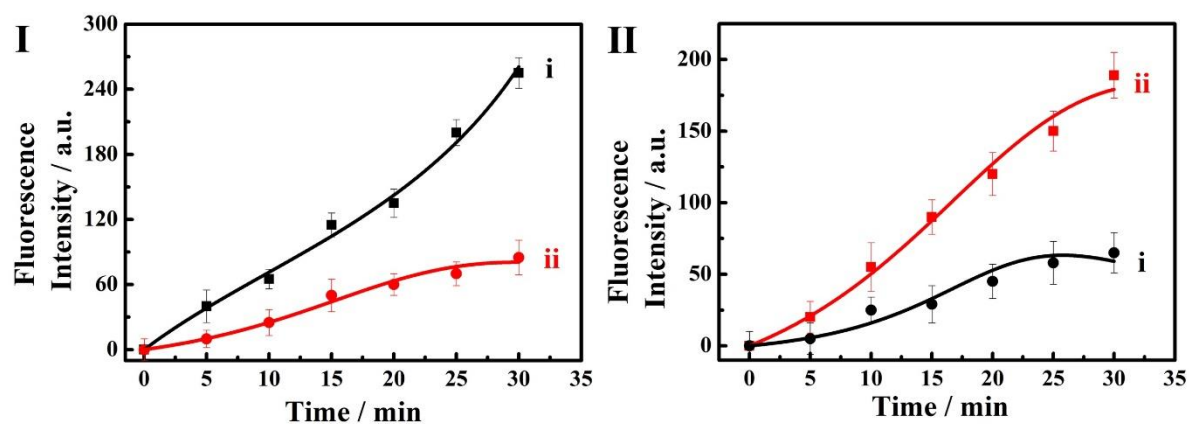


Figure S15. (A) Time-dependent release of the DOX-D from the MC-1 microcapsule driven by: (i) CDN “P” (ii) CDN “Q”. (B) Time-dependent release of the CPT-CMC from the MC-2 microcapsule driven by: (i) CDN “P” (ii) CDN “Q”. Error bars derived from $N=3$ experiments.

The sequences of the CDN “P” (from 5' to 3')

A: GATATCAGCGATACGATACAAACATTAGCATTAAACGTGCCTTAA

A': ACCCCTATCACGGTTTGTATCGTCACCCATGTTTCGTC

B: CTGCTCAGCGATACGATACAAACAATCCTTAA

B': GCATTCAGGTGTTTGTATCGTCACCCATGTTACTCT

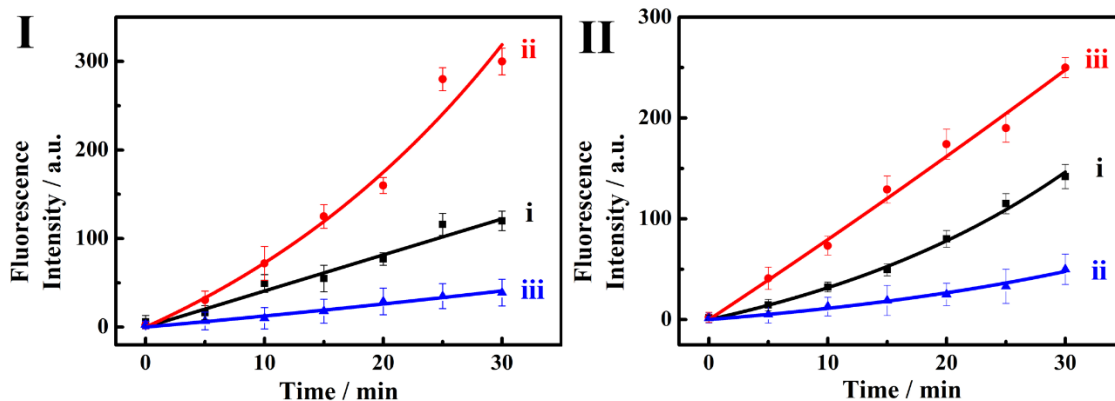


Figure S16. (I) Time-dependent release of the DOX-D from the MC-1 microcapsule driven by: (i) CDN “S” (ii) CDN “X” (iii) CDN “Y” in the presence of 10% fetal bovine serum (FBS). (II) Time-dependent release of the CPT-CMC from the MC-2 microcapsule driven by: (i) CDN “S” (ii) CDN “X” (iii) CDN “Y”. Error bars derived from $N=3$ experiments.

The dots in Figure S16, panel I and II represent the time-dependent fluorescence changes of the released drugs stimulated by the different CDNs. The solid line correspond to the fit of the experimental data to a first-order drug release profile¹ ($r=0.9845$ for MC-1 and $r=0.9952$ for MC-2). The results are very similar to the drug released profiles observed in pure buffer (*cf.* Figure 3). The minute deviation of some of the curves from linearity might originate from the non-specific adsorption of proteins to the microcapsules or CDNs constituents that might perturb slightly the drug release processes.

REFERENCE

1. Peng, X. S.; Zhou, Y. F.; Han K.; Qin, L. Z.; Dian, L. H.; Pan, X. G.; Wu, C. B.; Characterization of Cubosomes as a Targeted and Sustained Transdermal Delivery System for Capsaicin. *Drug Design, Development and Therapy*. **2015**, 9, 4209-4218.

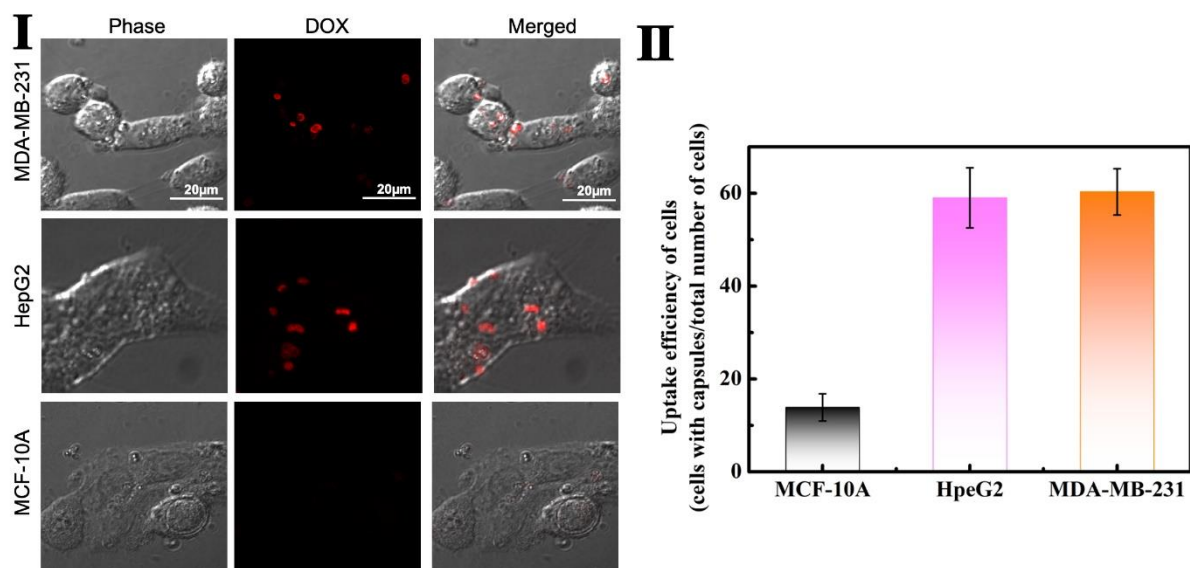


Figure S17. (I) Confocal microscopy images of MDA-MB-231, HepG2 and MCF-10A cells treated with DOX-D loaded microcapsules for 3 hours. (II) Statistical analysis corresponding to the cellular permeation of DOX-D loaded microcapsules. Data analyzed from $n=3$ signed domains. Error bars derived from $N=3$ experiments.

Synthesis and characterization of NMOFs-1 and NMOFs-2

The detailed preparation of the stimuli-responsive drug loaded UiO-68 NMOFs is detailed in Figure S18. It involves the primary transformation of the amine functionalities into azide units by the reaction of the NMOFs with tert-butyl nitrite (tBuONO) and azidotrimethylsilane (TMSN₃). The amino-functionalized nucleic acids (7) or (8) were coupled to dibenzocyclooctyne-sulfo-N-hydroxysuccinimidyl ester (DBCO-sulfo-NHS). The resulting alkynyl-modified nucleic acid conjugates were reacted with the azide-modified NMOFs using the “click chemistry” principle to yield the nucleic acid (7)-modified NMOFs or the (8)-functionalized NMOFs. By measuring UV absorbance of the unbound DNA, we estimated that the loading of (7) and (8) in the NMOFs corresponded to 6.78 nmol mg⁻¹ and 6.03 nmol mg⁻¹. The (7)-modified NMOFs were loaded with doxorubicin, DOX and locked by hybridization of (7') with the (7)-modified NMOFs. Similarly, the (8)-functionalized NMOFs were loaded with camptothecin, CPT, and the loaded drug was locked in the pores of the NMOFs through hybridization of (8') with the (8)-modified NMOFs. The DOX-loaded and CPT-loaded NMOFs were characterized by SEM and TEM imaging, Figure S19, revealing a bipyramidal structure (ca. 500 nm diameter). The loadings of DOX or CPT in the respective NMOFs were evaluated by the unlocking of the (7)/(7')-protected DOX-loaded NMOFs or the (8)/(8')-gated CPT-loaded NMOFs with the strands L1, (9) and L2, (10) through the strand displacement of the duplexes (9)/(7') and (10)/(8'), respectively, Figure S18 (C). Using appropriate calibration curves, we estimated the loading of DOX and CPT in the respective NMOFs to be 57.8 nmol mg⁻¹ and 44.8 nmol mg⁻¹, respectively.

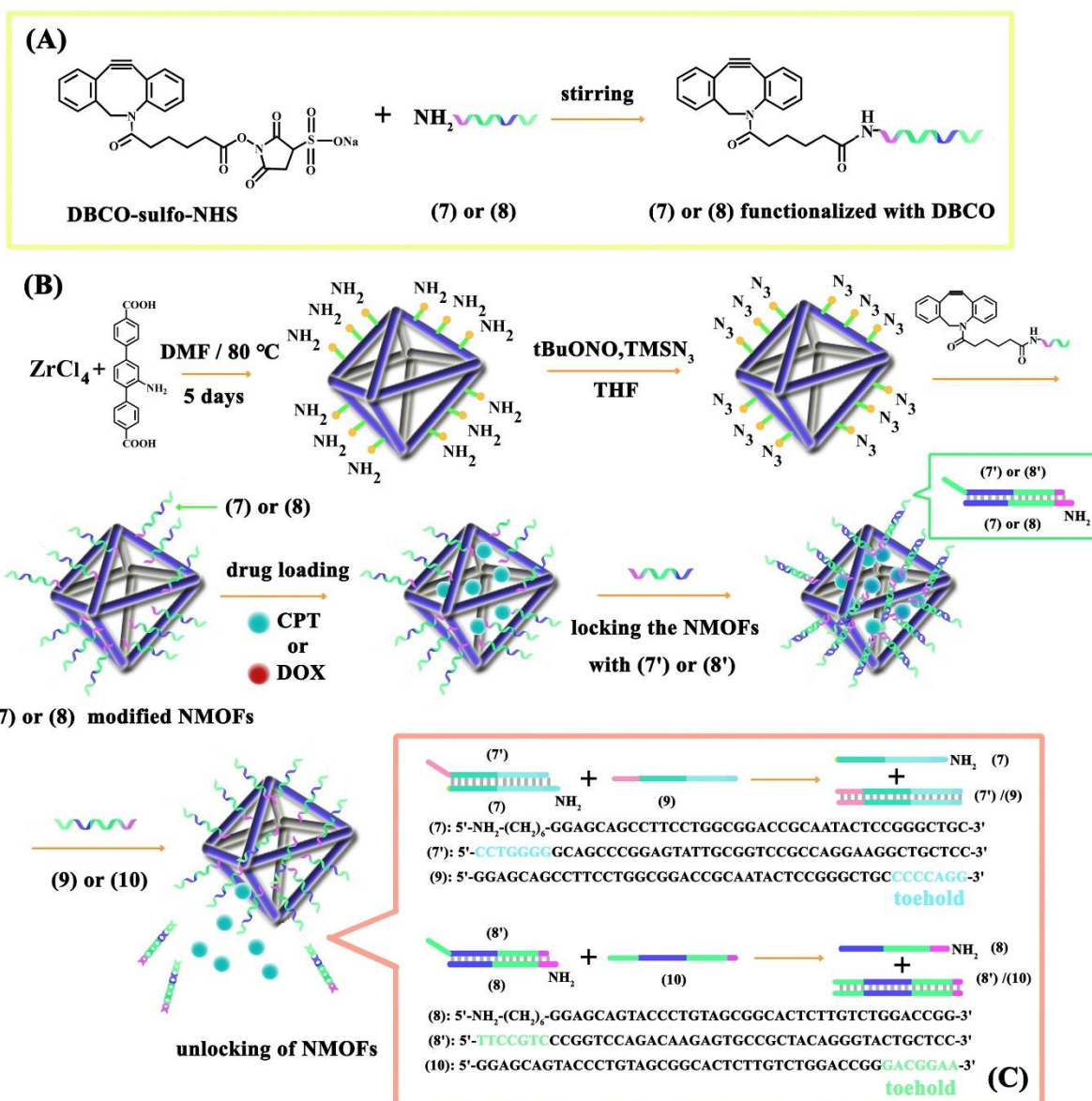


Figure S18. (A) Schematic preparation of DBCO-functionalized nucleic acid. (B) Schematic stepwise synthesis of the drug-loaded stimuli-responsive NMOFs. (C) The unlocking principle of (7)/(7')-protected DOX-loaded NMOFs-1 or the (8)/(8')-gated CPT-loaded NMOFs-2 with strand (9) or (10) through the strand displacement.

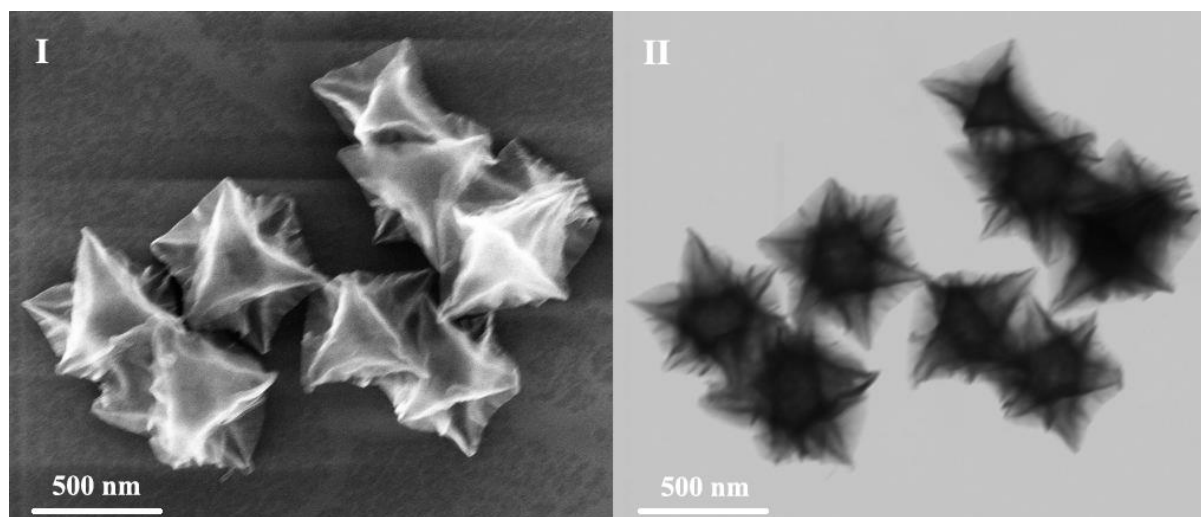


Figure S19. Panel I: SEM image of the NMOFs. Panel II: TEM image of the NMOFs.

Controlling the release of the DOX/CPT drugs from the NMOFs-1 and NMOFs-2 using the miRNAs-triggered reconfiguration of CDN “S” into CDN “X” or CDN “Y”

The application of the triggered constitutional dynamic networks to stimulate the controlled release of the DOX/CPT drugs from the NMOFs is presented in Figure S20 (for the primary characterization of the release of two different fluorescent dyes, see Figure S7 panel II, supporting information and accompanying discussion). CDN “S” includes the constituents AA', AB', BA', BB'. In the presence of the miRNA-155 (T₁), CDN “S” is reconfigured into CDN “X” where AA' is upregulated with the concomitant up-regulation of constituent BB' and the down-regulation of the constituent AB' and BA'. Similarly, subjecting CDN “S” to miRNA-124 (T₂), results in the reconfiguration of CDN “S” into CDN “Y”, where the constituent AB' is up-regulated with the concomitant up-regulation of BA' and the down-regulation of the constituent AA' and BB'. The composition of the equilibrated constituents in CDN “S”, “X” and “Y” was quantitatively evaluated by the Mg²⁺ ions-dependent DNAzyme units, associated with the different constituents, as described earlier (vide supra). The coupling of the T₁/T₂-triggered CDNs with the release of the drugs from the DOX/CPT-loaded NMOFs is achieved by introducing into the integrated CDNs/NMOFs assembled two hairpin structures H₁ and H₂ as auxiliary functional scaffolds. The constituent BB' cleaves hairpin H₁ resulting in the fragmented strand **L1**, (**9**). The released L1 unlocks the DOX-loaded NMOFs through the formation of the (**7**)/(**9'**) duplex, and results in the release of DOX. The constituents BA' cleaves hairpin H₂ and the fragmented strand **L2**, (**10**) unlocks the CPT-loaded NMOFs through the displacement of the duplex (**8**)/(**10'**), resulting in the release of CPT. The up-regulation of AA' or BA' upon the reconfiguration of CDN “S” into CDN “X” or CDN “Y”, in the presence of miRNA-155 or miRNA-124, is then anticipated to enhance the release of DOX or CPT from the respective NMOFs as compared to the release efficiencies from CDN “S”.

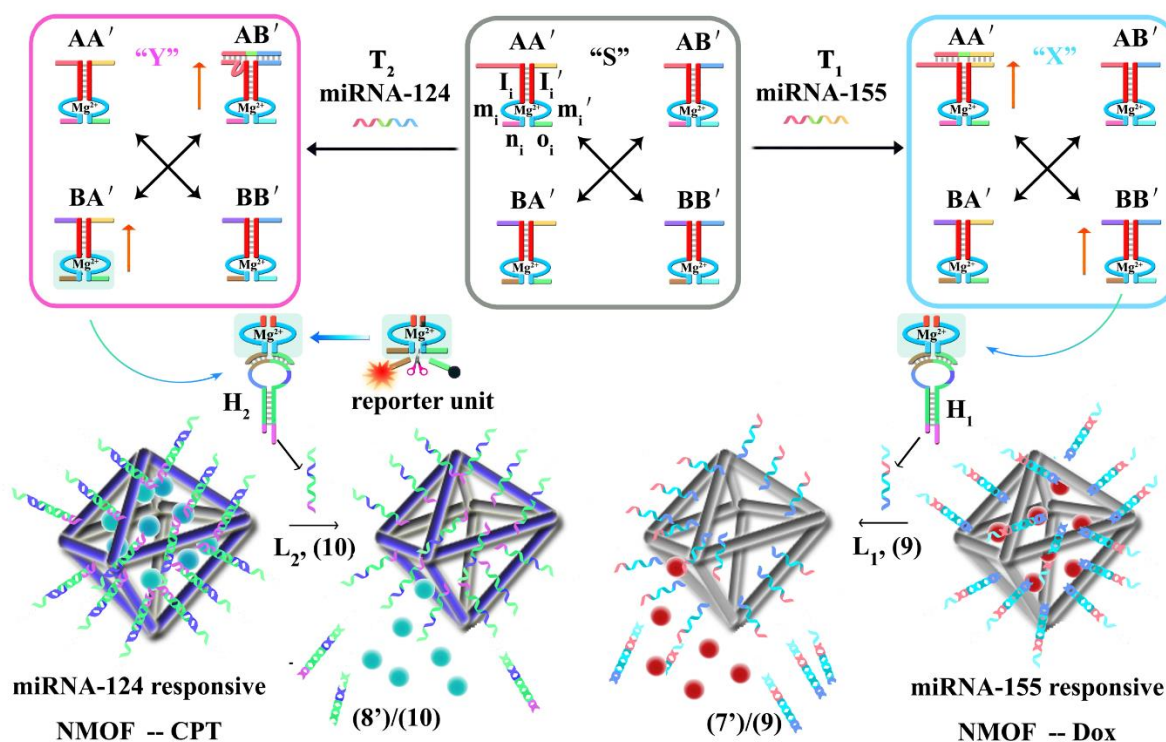


Figure S20. Scheme for the miRNA constitutional dynamic networks (CDNs)-guided release of loads from DNA-functionalized NMOFs. The miRNA triggered reconfiguration of CDN “S” to CDN “X” leads to the guided unlocking of DOX -loaded miRNA-155 responsive NMOF (NMOF-1) and the miRNA-124-triggered reconfiguration of CDN “S” to CDN “Y” leads to the guided unlocking of the CPT-CMC loaded miRNA-124 responsive NMOF (NMOF-2).

Direct miRNA release of the DOX-D or CPT-CMC from MC-1 and MC-2

(in the absence of CDNs)

To demonstrate the function of the CDNs in the amplified release of the drugs from the respective MC-1 and MC-2, we performed the following control experiments:

a) We engineered a microcapsule loaded with DOX-D, where the bridging units stabilizing the capsule coating include the complementary strand to miRNA-155, strand **(b)**, Figure S21 (A). These capsules were subjected to miRNA-155 at concentrations corresponding to 5 nM and 10 nM. Figure S21 (B) shows that at these concentrations no release of the drugs occurs. It should be noted that in the presence of the CDN “X” generated by the miRNA-155-driven reconfiguration of CDN “S”, effective release of DOX-D proceeds at these miRNA-155 concentrations, *cf.* Figure 6, panel I, in the main text.

b) We engineered a microcapsule loaded with CPT-CMC, where the bridging units stabilizing the capsule coating include the complementary strand to miRNA-124, strand **(p)**, Figure S22 (A). These capsules were subjected to miRNA-124 at concentrations corresponding to 5 nM and 10 nM. Figure S22 (B) shows that no release of CPT-CMC proceeds at these concentrations of miRNA-124. We note, however, that effective release of CPT-CMC from the capsules proceeds at these miRNA concentrations, the release of CDN “Y” generated by the miRNA-124 triggered reconfiguration of CDN “S” to CDN “Y”, *cf.* Figure 6, panel II, main text. These results clearly emphasize the function of the CDNs in the amplified release of the drugs from the respective microcapsules.

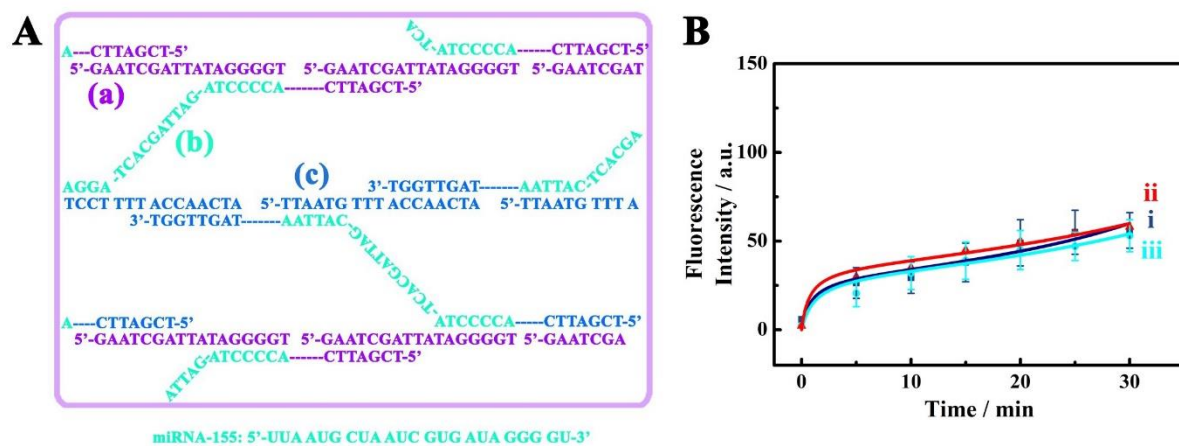


Figure S21. (A) Detailed sequences corresponding to the miRNA-155 complementary strand, (b)-bridged DNA shell components, comprising the miRNA-155-sensitive microcapsules. (B) Time-dependent DOX-D release from MC-1 in the presence of (i) 5 nM miRNA-155; (ii) 10 nM miRNA-155; (iii) in the absence of miRNA-155. Error bars derived from $N=3$ experiments.

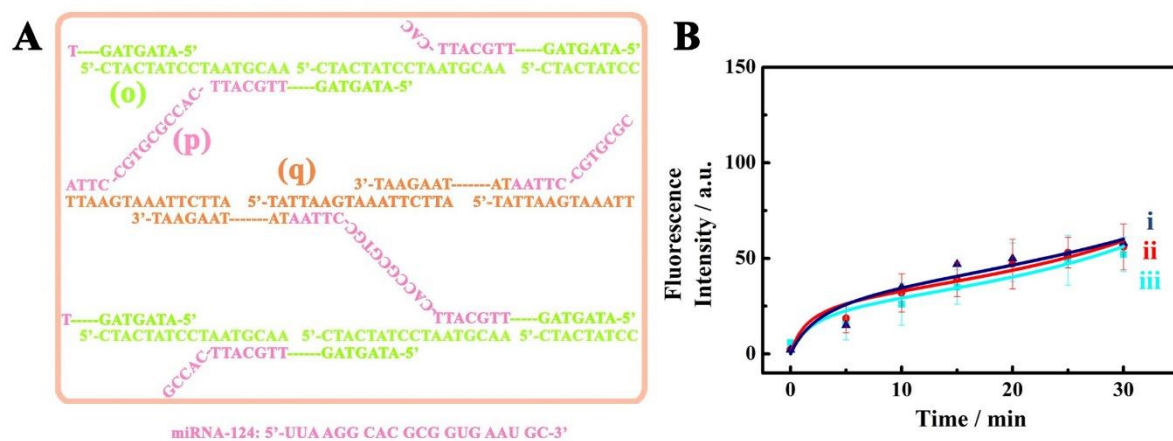


Figure S22. (A) Detailed sequences corresponding to the miRNA-124 complementary strand (p)-bridged DNA shell components, comprising the miRNA-124-sensitive microcapsules. (B) Time-dependent CPT-CMC release from MC-2 in the presence of (i) 5 nM miRNA-124; (ii) 10 nM miRNA-124; (iii) in the absence of miRNA-124. Error bars derived from $N=3$ experiments.

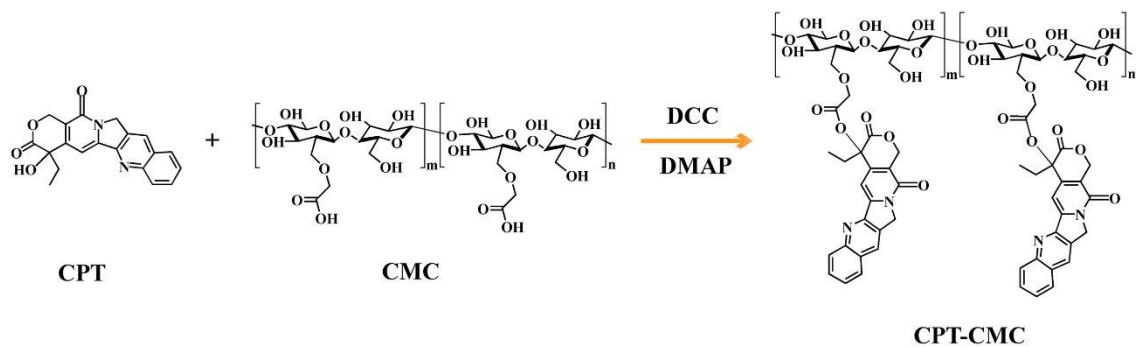


Figure S23. The preparation of camptothecin-conjugated carboxymethyl cellulose, CPT-CMC.

REFERENCES

(S1) He, C. B.; Lu, K. D.; Liu, D. M.; Lin, W. B. Nanoscale Metal-Organic Frameworks for the Co-Delivery of Cisplatin and Pooled siRNAs to Enhance Therapeutic Efficacy in Drug-Resistant Ovarian Cancer Cells. *J. Am. Chem. Soc.* **2014**, *136*, 5181-5184.